JOURNAL OF CATALYSIS **164,** 82–93 (1996)
ARTICLE NO. 0365

A Surface Science Study of the Hydrogenation and Dehydrogenation Steps in the Interconversion of C_6 Cyclic Hydrocarbons on Ni(100)

Sariwan Tjandra and Francisco Zaera[1]

Department of Chemistry, University of California, Riverside, CA 92521

Received April 15, 1996; revised July 29, 1996; accepted July 30, 1996

The thermal chemistry of C_6 cyclic hydrocarbons (cyclohexane, cyclohexene, benzene, 1,3- and 1,4-cyclohexadienes, 1-methyl-1-cyclohexene, and toluene) and halo hydrocarbons (iodo cyclohexane, iodo benzene, and 3-bromo cyclohexene) on Ni(100) surfaces has been studied under ultrahigh vacuum conditions by using temperature-programmed desorption (TPD). Cyclohexane was found to only desorb molecularly from the surface, but this is because of the dynamic nature of TPD experiments, and is therefore not an indication of the inability of nickel to activate the adsorbed molecules. Indeed, cyclohexyl groups, which are the first expected intermediates after the initial C–H bond scission and which were prepared via the thermal treatment of adsorbed iodo cyclohexane, were shown to undergo a facile β-hydride elimination step to yield first cyclohexene and ultimately benzene, and to concurrently follow a reductive elimination path with surface hydrogen to produce cyclohexane. Cyclohexene was found to dehydrogenate easily to benzene and to not hydrogenate to any significant extent even if atomic hydrogen is present on the surface (again, because the dynamic nature of TPD favors molecular desorption instead). The allylic intermediate expected to form during the dehydrogenation of cyclohexene to cyclohexadiene was prepared by thermal decomposition of 3-bromo cyclohexene and studied by TPD as well, and the remaining hydrogenation and dehydrogenation steps were probed by characterizing the thermal chemistry of the other compounds listed above.

1. INTRODUCTION

The adsorption and thermal chemistry of cyclic compounds such as cyclohexane, cyclohexene, cyclohexadiene, and benzene on transition metal surfaces have been studied extensively in the past by using surface-sensitive techniques such as LEED, HREELS, TPD, ARUPS, and XPS (1–23). In particular, the molecular adsorption of different cyclic compounds has been reported on Ni(111) (1–11), Ni(100) (2–6, 12), Pt(111) (13–18), Ru(001) (19, 20), Pd(110) (21–23), and Cu(100) (24). Cyclohexane has been found to adsorb molecularly at low temperatures in most instances (<200 K), probably by keeping its chair configuration. Molecular desorption of this cyclohexane is seen in some cases upon heating of the surface, but its dehydrogenation to benzene is preferred in others; the resulting benzene then either desorbs or decomposes further to yield hydrogen and adsorbed carbon. Both cyclohexene and allylic C_6H_9 species have been proposed as intermediates in the conversion of cyclohexane to benzene on some surfaces. In general, cyclohexene adsorption below 100 K is also associative, but the molecule almost always dehydrogenates at higher temperatures to form benzene, some of which desorbs if it is produced at high enough converages while the rest decomposes to dehydrogenated surface carbon species. Similarly, both 1,3- and 1,4-cyclohexadienes convert readily to benzene on all metal surfaces studied so far. Benzene chemisorbs molecularly at low temperatures with a molecular geometry that changes, from parallel to the surface at low coverages (in a predominantly π-bonded configuration that involves minimal or no rehybridization) to a tilted arrangement as the packing density on the surface is increased. Again, molecular desorption and/or decomposition occurs upon heating in this case depending on the initial coverage.

The use of alkyl halides as precursors for the preparation of alkyl groups on transition metal surfaces under vacuum has also become a common procedure to generate many hydrocarbon fragments relevant to catalytic processes (25–28). Most alkyl groups have shown to undergo two specific pathways preferentially, a β-hydride elimination step to yield the corresponding olefin (unless no β-hydrogens are available in the molecule) and a reductive recombination with surface hydrogen atoms (if available) to produce alkanes.

As part of our continuing studies on the chemistry of hydrocarbons on metal surfaces (25, 29–41), in this paper we report temperature-programmed desorption (TPD) results from experiments with various cyclic compounds on Ni(100). It was found here that cyclohexane adsorbs molecularly on that surface, and that multilayer and monolayer cyclohexane desorption occur at about 140 and 180 K, respectively. In addition to molecular desorption, the thermal activation of adsorbed cyclohexene leads to the formation of both benzene and a small amount of cyclohexane, and in

[1] Corresponding author.

0021-9517/96 $18.00

the presence of coadsorbed deuterium some H–D exchange leading to the formation of monodeutero-cyclohexene and cyclohexane is detected as well. Interestingly, though, the dehydrogenation of 1-methyl-1-cyclohexene does not lead to the desorption of any toluene. For low converages of 1,3- or 1,4-cyclohexadiene only total decomposition to hydrogen and surface carbon occurs, but at higher coverages dehydrogenation to benzene is also seen. In terms of the halo compounds, the fact that the thermal activation of iodo cyclohexane leads to the formation of cyclohexane, cyclohexene, and benzene suggests that a cyclohexyl species is a likely intermediate in the conversion of cyclohexane to cyclohexene. Analogous desorption of benzene and cyclohexene (in addition to hydrogen) are observed in the case of 3-bromo cyclohexene, indicating that cyclohexenyl moieties are also expected to form during the conversion of cyclohexene to cyclohexadiene. Finally, only hydrogen and benzene desorption is seen from Ni(100) surfaces dosed with various amounts of iodo benzene.

2. EXPERIMENTAL

The ultrahigh vacuum chamber used in these studies has been described in detail previously (29, 33, 39). Briefly, it has a base pressure below 1×10^{-10} Torr and is equipped with instrumentation for temperature-programmed desorption (TPD), X-ray photoelectron (XPS), static secondary-ion mass (SSIMS), Auger electron (AES), and ion scattering (ISS) spectroscopies. All the TPD experiments were performed by using a mass quadrupole with an electron impact ionizer located inside an enclosed compartment with two small apertures at the front and back for gas sampling and exit to the quadrupole rods, respectively. The nickel is positioned at about 1 mm from the front aperture to allow for the selective detection of the gases that desorb from the front surface. Desorption of up to 15 different masses could be followed simultaneously with this setup by using an interfaced computer. The partial pressures from the TPD experiments are reported in arbitrary units, but they are all related to a common scale given by the bar included in each of the figures. A heating rate of about 10 K/s was used in all runs.

The nickel single crystal was cut and polished in the (100) direction by using standard procedures, mounted in a manipulator capable of both resistively heating to about 1300 K and cooling to liquid nitrogen temperatures, and cleaned before each experiment by cycles of argon ion sputtering and annealing until no impurities were detected by either AES or XPS. The temperature was measured by a chromel–alumel thermocouple spot-welded to the side of the crystal, and continuously regulated using a commercial precision temperature controller. The organic compounds were all purchased from Aldrich (>99% purity), and were distilled by freeze–pump–thaw cycles and checked by mass spectrometry before use. Both ultrahigh purity hydrogen and deuterium were obtained from Matheson Gas Products and used as supplied. The gas dosing was done in all cases by backfilling of the vacuum chamber using leak valves, and the pressures were measured by using a nude ionization gauge. Gas exposures are reported in langmuirs ($1\ \mathrm{L} = 1 \times 10^{-6}$ Torr · s), uncorrected for differences in ion gauge sensitivities.

3. RESULTS

Temperature-programmed desorption (TPD) data were obtained for the various cyclic C_6 hydrocarbons listed above, which were initially adsorbed on the Ni(100) surface at temperatures below 100 K. The TPD from stable compounds will be described first. The left panel of Fig. 1 summarizes the spectra from 3.0 L of cyclohexane adsorbed on clean Ni(100) at 90 K, an exposure that leads to a coverage well below saturation. Only molecular cyclohexane and a small amount of hydrogen desorb in that case. The main hydrogen signal in the TPD seen at 375 K originates

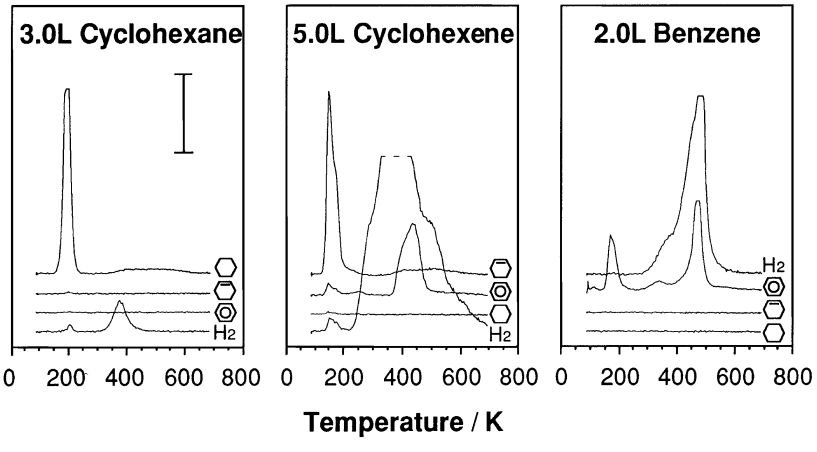

FIG. 1. H_2, cyclohexane, cyclohexene, and benzene TPD spectra from Ni(100) surfaces dosed with 3.0 L of cyclohexane (left), 5.0 L of cyclohexene (center), and 2.0 L of benzene (right) at 90 K.

from adsorption from the background, and the small peak at 200 K corresponds to cracking of the cyclohexane in the ionizer; no decomposition was seen for this molecule in these TPD experiments (neither cyclohexene nor benzene were detected). Monolayer cyclohexane desorption is seen at 200 K, but additional cyclohexane desorption from physically adsorbed multilayers is also observed at 140 K after higher doses (not shown). Assuming a preexponential factor of $10^{13}\,s^{-1}$ (42), the activation energies for the multilayer and monolayer molecular desorption are estimated to be about 8.5 and 12.5 kcal/mole, respectively.

The center panel of Fig. 1 shows TPD spectra from a surface dosed with 5.0 L of cyclohexene at 90 K. In addition to the desorption of molecular cyclohexene and hydrogen, benzene was also detected in this case. Multilayer and monolayer cyclohexene desorption occurs at 145 and 180 K, respectively, and hydrogen desorption takes place in a broad temperature range between 230 to 600 K. The large amount of hydrogen that is produced in this case (the signal went out of range in these experiments) mainly originates from the dehydrogenation of cyclohexene to benzene, which desorbs in two stages at about 250 and 435 K (the signals at 145 and 180 K in that trace are most likely the product of cyclohexene cracking in the ionizer). The peak at 435 K accounts for about 90% of the total benzene yield, but since the spectra from cyclohexene are similar to those from direct adsorption of benzene, the detection of this product is most likely desorption-limited; benzene formation from cyclohexene probably occurs below 200 K.

The TPD spectra for adsorbed benzene shown in the right panel of Fig. 1 are in good agreement with those reported in literature [5]. Most of the molecular benzene desorbs in two peaks, about 165 and 480 K which, according to the previous reports, correspond to tilted and flat-lying benzene adsorption states, respectively. The latter peak develops an additional small shoulder around 340 K at high coverages, and some benzene decomposition is also detected by the formation of hydrogen, which desorbs mainly about 475 K (a small shoulder also appears around 385 K). No cyclohexene nor cyclohexane were detected from thermal activation of this molecule.

In order to study the effect of surface hydrogen on the chemistry of adsorbed cyclohexene, experiments were done on surfaces where either hydrogen or deuterium was dosed before cyclohexene adsorption. The left panel of Fig. 2, which shows the TPD spectra obtained after the sequential dosing of 2.0 L H_2 and 5.0 L cyclohexene, indicates that hydrogen, cyclohexene, and a small amount of cyclohexane are the only desorbing products detectable from this system. Dehydrogenation to benzene is almost completely inhibited by the coadsorbed hydrogen, but hydrogenation to cyclohexane does not occur to any significant extent (a little is seen around 220 K), and molecular desorption about 180 K and decomposition to carbon and hydrogen (which

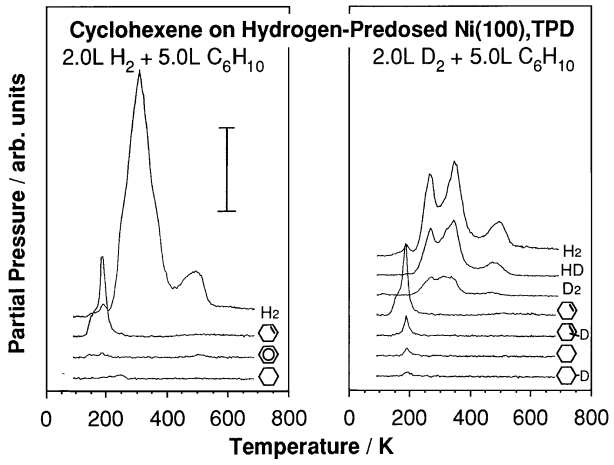

FIG. 2. Left: H_2, cyclohexene, benzene, and cyclohexane TPD spectra from a Ni(100) surface dosed sequentially with 2.0 L of hydrogen and 5.0 L of cyclohexane. Right: H_2, HD, D_2, normal- and monodeutero-cyclohexene, and normal- and monodeutero-cyclohexane TPD from a Ni(100) surface dosed sequentially with 2.0 L of deuterium and 5.0 L of cyclohexene. All dosings were done at 90 K.

desorbs mostly around 300 K) dominates the chemistry in this case. The TPD spectra obtained from the case of 2.0 L of deuterium coadsorbed with 5.0 L of cyclohexene (right panel of Fig. 2) supports that conclusion, and, in addition, indicates that some H–D exchange occurs within the cyclohexene itself, because monodeutero-cyclohexene desorption is also observed at 185 K. The H_2, HD, and D_2 TPD displays three peaks, the two features seen before around 350 and 500 K, and an additional peak about 250 K that was unresolved in the hydrogen coadsorption case and that originates from the preadsorbed deuterium. The similar relative intensities of these peaks in the three traces and the significant desorption of deuterium at high temperatures corroborate that some H–D scrambling does take place in this system. Finally, as in the case of hydrogen coadsorption, only a small amount of cyclohexane (some H–D exchanged) is detected.

Figure 3 shows a series of benzene (a, left) and H_2 (b, right) thermal desorption spectra obtained after dosing different amounts of 1,3-cyclohexadiene on Ni(100) at 90 K. No cyclohexane, cyclohexene, or cyclohexadiene were detected as significant desorption products from the nickel surface in these experiments. In fact, only total decomposition to hydrogen is seen at coverages below 1.0 L, where no benzene is produced. As the exposure increases to 2.0 L, however, the dehydrogenation reaction that generates benzene is turned on, and this product begins to appear in the spectra as a large peak about 210 K and a small feature at 420 K. As the initial dose is increased further to 3.0 L, the low temperature benzene peak shifts to about 170 K, whereas the high temperature feature grows and moves to 485 K. These changes parallel those seen for adsorbed

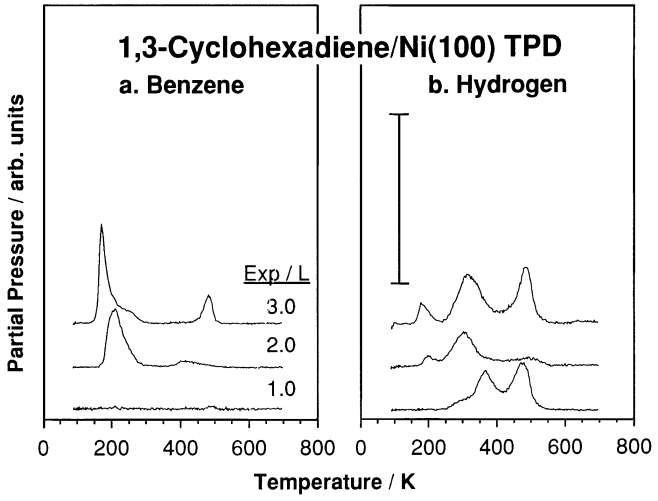

FIG. 3. Benzene (a, left) and hydrogen (b, right) TPD spectra from 1,3-cyclohexadiene adsorbed on Ni(100) as a function of initial exposure. The dosing was done at 90 K in all cases, and a heating rate of 10 K/s was used.

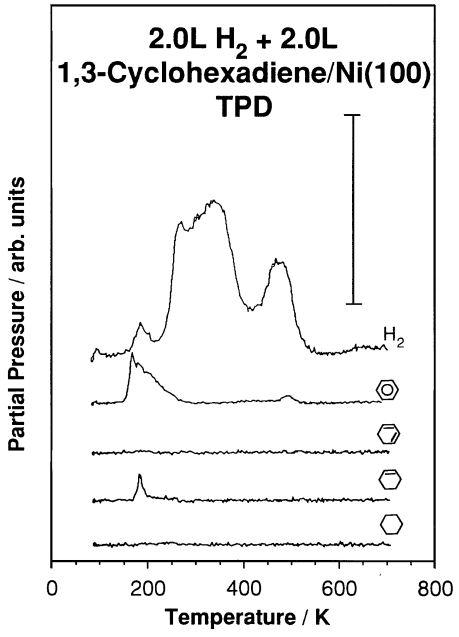

FIG. 4. H_2, benzene, cyclohexadiene, cyclohexene, and cyclohexane TPD spectra from a Ni(100) surface dosed sequentially with 2.0 L of hydrogen and 2.0 L of 1,3-cyclohexadiene at 90 K.

benzene on clean Ni(100), indicating that the dehydrogenation of 1,3-cyclohexadiene most likely occurs below 170 K, and thus the benzene desorption below 200 K and above 400 K are in this case tentatively assigned to tilted and flat-lying benzene, respectively, all produced at low temperatures. In addition, a small amount of molecular cyclohexadiene also desorbs after the high exposures about 165 K (not shown). With respect to the hydrogen TPD, the spectrum from 1.0 L 1,3-cyclohexadiene shows two main peaks at 365 and 475 K and a shoulder around 320 K. The low temperature desorption feature appears in the same range as for H_2 desorption from hydrogen dosed on clean Ni(100) and is limited by the rate of atomic hydrogen recombination on the surface, but the higher temperature peaks must be controlled by surface decomposition reactions. After a 2.0 L exposure the total hydrogen yield decreases at the expense of benzene formation, and the temperature of the desorption maxima changes so the first peak shifts to 305 K and becomes dominant and the second shoulder moves to higher temperatures (495 K) and becomes quite small. At higher coverages, where benzene desorption about 485 K becomes significant, the yield of H_2 production increases, and the desorption splits into two significant peaks around 315 and 475 K (the third at 175 K comes from cracking of benzene in the ionizer); it is quite likely that at this stage the low temperature H_2 peak is mostly the result of the initial cyclohexadiene dehydrogenation while that at higher temperatures originates from decomposition of the benzene formed (compare this trace to the data in the right panel of Fig. 1).

The effect of the presence of coadsorbed hydrogen on the surface chemistry of 1,3-cyclohexadiene is illustrated by the spectra in Fig. 4. There it can be seen that the dehydrogenation process that yields benzene is still active, even though it no longer dominates the overall chemistry, and that a small amount of cyclohexene (but not cyclohexane) is also produced. Cyclohexene desorbs in this case at 185 K, about the same temperature as when cyclohexene is dosed directly on clean Ni(100), so this process could be desorption limited. Some hydrogen from hydrocarbon decomposition desorbs in broad peaks centered about 280, 340, and 485 K.

Like 1,3-cyclohexadiene, 1,4-cyclohexadiene decomposes completely at low coverages on Ni(100). Indeed, the data in Fig. 5 indicate that total decomposition occurs

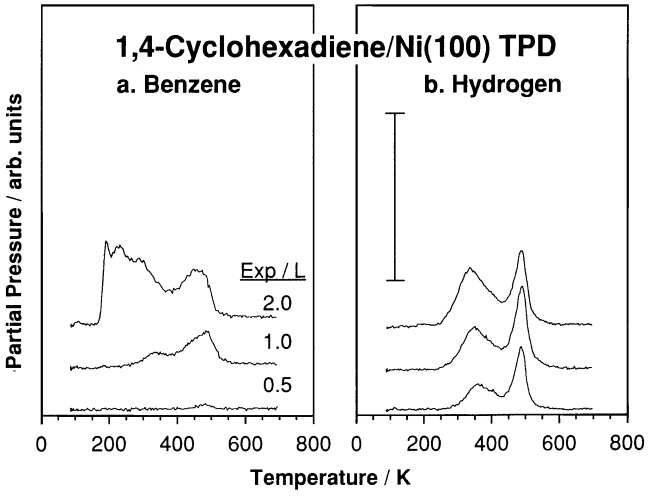

FIG. 5. Benzene (a, left) and hydrogen (b, right) TPD spectra from 1,4-cyclohexadiene adsorbed on Ni(100) at 90 K as a function of initial exposure.

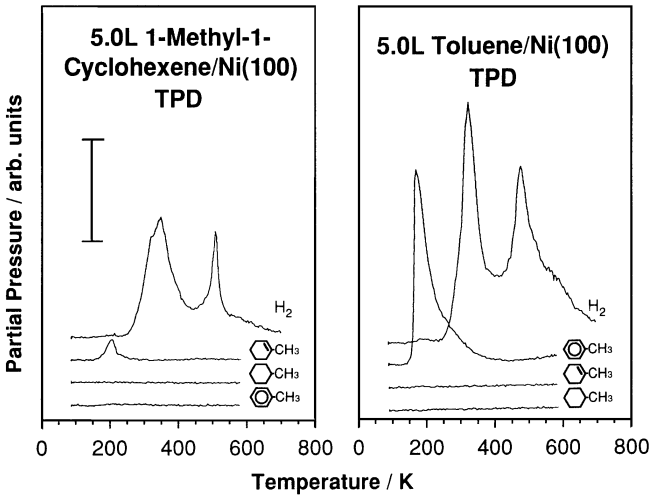

FIG. 6. H_2, methyl cyclohexane, methyl cyclohexene, and toluene TPD spectra from Ni(100) surfaces dosed with either 5.0 L of 1-methyl-1-cyclohexene (left) or 5.0 L of toluene (right) at 90 K.

after a 0.5 L dose (where only hydrogen desorbs), but some benzene is also detected about 340 and 500 K at higher coverages (>1.0 L exposures). The benzene TPD features become larger and broader and appear at higher temperatures than those seen for either 1,3-cyclohexadiene or benzene (Fig. 5a), indicating that the dehydrogenation of 1,4-cyclohexadiene is more difficult than in the cyclohexene or 1,3-cyclohexadiene cases. Hydrogen desorption occurs at 360 and 490 K for the 1.0 L exposure, and the lower temperature peak increases in intensity and shifts slightly to lower temperature with increasing exposure while the high temperature feature remains at about the same temperature for the different exposures (Fig. 5b). The overall hydrogen yield increases by about a factor of two as the exposure is increased from 0.5 to 3.0 L.

Unlike in the case of cyclohexene, the TPD of 1-methyl-1-cyclohexene displayed in the left panel of Fig. 6 shows no significant desorption of the aromatic (toluene) product. Below saturation only a small amount of molecular desorption is seen about 200 K, a temperature that corresponds to an activation energy of about 12.5 kcal/mol, but at higher coverages the multilayer desorbs around 165 K, and decomposition of 1-methyl-1-cyclohexene generates hydrogen, which desorbs at about 350 and 505 K. The fact that no toluene is detected in this case suggests that the initial decomposition step involves the methyl group and therefore follows a different route than cyclohexene. It should be pointed out, however, that if a small amount of toluene were to form in this case, it would most likely decompose completely to surface carbon and hydrogen [5]; molecular desorption from 5.0 L of toluene adsorbed on the nickel surface is seen as a sharp peak about 180 K, but some decomposition to hydrogen, which desorbs at 340 and 490 K, is also observed (right panel of Fig. 6). No hydrogenation to methyl cyclohexene (in the case of toluene) or methyl cyclohexane was detected in these experiments.

In an attempt to identify possible surface intermediates during the dehydrogenation reactions discussed above, TPD experiments were also performed with iodo cyclohexane, iodo benzene, and 3-bromo cyclohexene. The carbon-halogen bond in alkyl halides has been shown to cleave preferentially and at temperatures below 200 K, so alkyl groups can be easily generated this way (25–28, 35–37). As an example of this, the thermal chemistry of cyclohexyl groups as a function of exposure is illustrated by the TPD of iodo cyclohexane shown in Fig. 7. Unlike cyclohexane or cyclohexene, the thermal activation of iodo cyclohexane leads to the formation of all cyclohexane, cyclohexene, and benzene. The desorption of H_2 is examined in Fig. 7a. A complex trace is seen after a 2.0 L iodo cyclohexane dose, with major hydrogen peaks at 360 and 490 K which shift to about 430 and 510 K at higher coverages, and an additional peak at about 330 K also develops at 5.0 L and above; the overall hydrogen yield decreases by about 20% as the exposure changes from 2.0 to 10.0 L. The TPD spectra for benzene (Fig. 7b) shows the initial development of a small peak

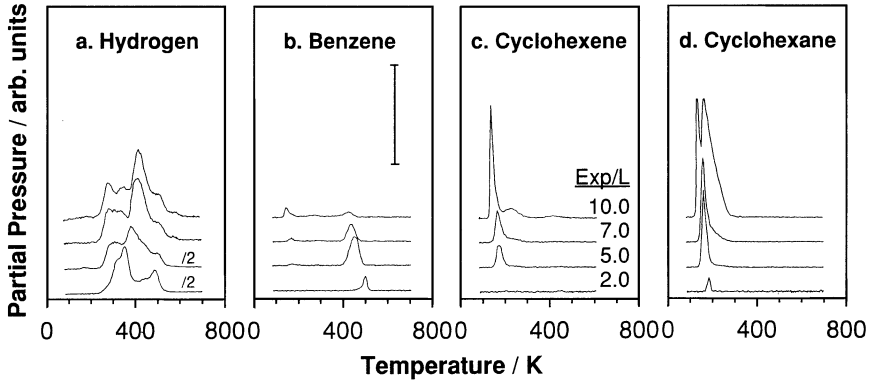

FIG. 7. H_2 (a), benzene (b), cyclohexene (c), and cyclohexane (d) TPD spectra from iodo cyclohexane adsorbed on Ni(100) at 90 K as a function of initial exposure.

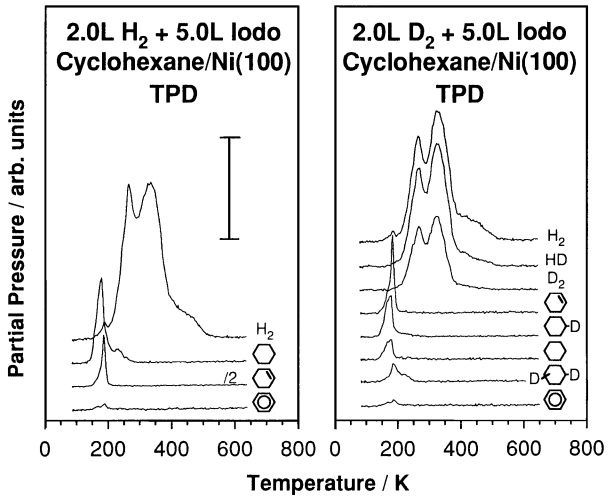

FIG. 8. Left: H_2, cyclohexane, cyclohexene, and benzene TPD spectra from a Ni(100) surface dosed sequentially with 2.0 L of hydrogen and 5.0 L of iodo cyclohexane. Right: H_2, HD, D_2, cyclohexene, normal-, monodeutero-, and dideutero-cyclohexane, and benzene TPD spectra from a Ni(100) surface dosed sequentially with 2.0 L of deuterium and 5.0 L of iodo cyclohexane. All dosings were done at 90 K.

about 500 K starting at 2.0 L that increases in intensity and shifts to about 450 K at 5.0 L. At even higher coverages (10.0 L) the benzene yield decreases, but the temperature of desorption continues to shift down to about 420 K, and a second low temperature peak appears around 150 K (which may be associated with cracking of either cyclohexane or cyclohexene in the mass spectrometer ionizer). The cyclohexene TPD (Fig. 7c) shows no detectable signal at iodo cyclohexane doses below 2.0 L, but a small amount of cyclohexene is seen at 175 K after a 5.0 L exposure, and more is produced at lower temperatures at higher coverages. Finally, some cyclohexane desorption was also detected (Fig. 7d), only a small amount around 190 K at low iodo cyclohexane doses, but significantly more as the doses increases from 2.0 to 5.0 or 7.0 L, in which case the TPD peak grows and shifts to 160 K. The use of even larger exposures induces the growth of an additional low temperature sharp peak at 140 K, probably related to either alkyl direct displacement or radical formation from the iodo cyclohexane molecule, as reported in order cases [39]. The overall yield for cyclohexane formation is about two times that of cyclohexene at either 5.0 or 7.0 L, and no molecular desorption is seen after exposures below 10.0 L.

In order to pin down the mechanism for the hydrogenation of cyclohexyl groups to cyclohexane, experiments were also performed on surfaces where either hydrogen or deuterium was dosed before the chemisorption of iodo cyclohexane. When 2.0 L of H_2 is adsorbed on the nickel surface prior to iodo cyclohexane dosing (left panel of Fig. 8), the formation of benzene is almost entirely suppressed at the expense of cyclohexene formation, which desorbs at about 185 K. Interestingly, though, the cyclohexane yield stays about the same as when there is no coadsorbed hydrogen on the surface, so the ratio of cyclohexane to cyclohexene reaches a value of about 0.5 in the hydrogen coadsorption case. This suggests that both the hydrogenation and the dehydrogenation of cyclohexyl moieties are facile reactions, and that what coadsorbed hydrogen does is inhibit the further dehydrogenation of the resulting cyclohexene to benzene; this effect was indeed already observed in the experiments illustrated in Fig. 2. In the case of deuterium coadsorption with iodo cyclohexane (right panel of Fig. 8b), the hydrogenation products and normal, monodeutero-, and dideutero-cyclohexane, which desorbs at 170, 180, and 185 and 220 K, respectively, whereas the dehydrogenation reaction produce only normal cyclohexene around 185 K (no significant benzene desorption is observed here either). It is important to note that the formation of dideutero-cyclohexane, which requires the H–D exchange of at least one hydrogen in the original cyclohexyl ring, is seen at a higher temperatures (185 and 220 K) than the rest.

The desorption of hydrogen and benzene from Ni(100) surfaces dosed with various exposures of iodo benzene are shown in Fig. 9. After a 3.0 L iodo benzene dose, H_2 desorption is seen at about 300 and 510 K (Fig. 9a). The intensity of the low temperature peak decreases only slightly as the exposure changes from 3.0 to 5.0 L, but it goes down to about half the original size at 7.0 L, and the peak maximum shifts to lower temperatures at higher coverages, from 300 to about 285 K. The high temperature H_2 peak, on the other hand, decreases in size, and two additional features grow about 540 and 610 K. Benzene desorption (Fig. 9b) is seen initially only at about 445 K (for 3.0 L of iodo benzene), but a second peak appears at 225 K after a 4.0 L dose. As the initial dose increases to 7.0 L, the high temperature

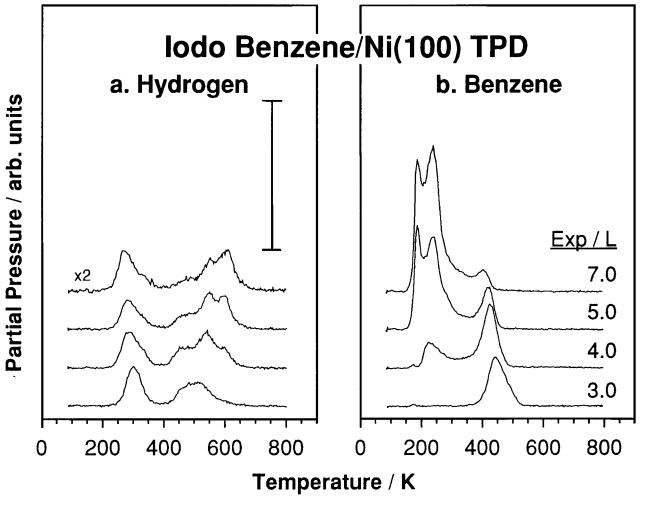

FIG. 9. Hydrogen (a, left) and benzene (b, right) TPD spectra from iodo benzene adsorbed on Ni(100) at 90 K as a function of initial exposure.

benzene peak decreases to about half of its initial size and a large amount of benzene desorbs at 190 and 245 K, and at even higher exposures (10.0 L) the sharp peak at 185 K becomes dominant. The overall yield for benzene formation increases by about four times in going from 3.0 L to 10.0 L of initial iodo benzene.

The presence of hydrogen on the surface before iodo benzene dosing leads to the desorption of benzene in one single sharp peak about 190 K (Fig. 10, left). No other reactions were observed in this case, only the direct hydrogenation of the phenyl groups with the coadsorbed hydrogen to form benzene, and, furthermore, none of the high temperature benzene features were seen here at all. Hydrogen desorption is seen in two main peaks at 255 and 355 K and a third smaller feature around 480 K which could be associated with hydrocarbon decomposition. Coadsorption of deuterium, instead of hydrogen, generates monodeuterobenzene, as expected (Fig. 10, right), but about 40% of normal benzene is produced as well, most likely via the recombination of the phenyl groups with hydrogen from background adsorption. Also, a small kinetic isotope effect is manifested in this case by the fact that C_6H_5D desorbs at about 5 K higher temperature than C_6H_6. No evidence for extensive H–D exchange between benzene and surface deuterium was seen here, since no appreciable dideuterobenzene was detected (small features are nevertheless seen around 280 and 480 K), and no significant deuterium desorption was seen at high temperatures.

Finally, in order to emulate the surface chemistry of the allylic cyclic intermediate expected to form during the dehydrogenation of cyclohexene, a few TPD experiments were also done with 3-bromo cyclohexene. The left panel of

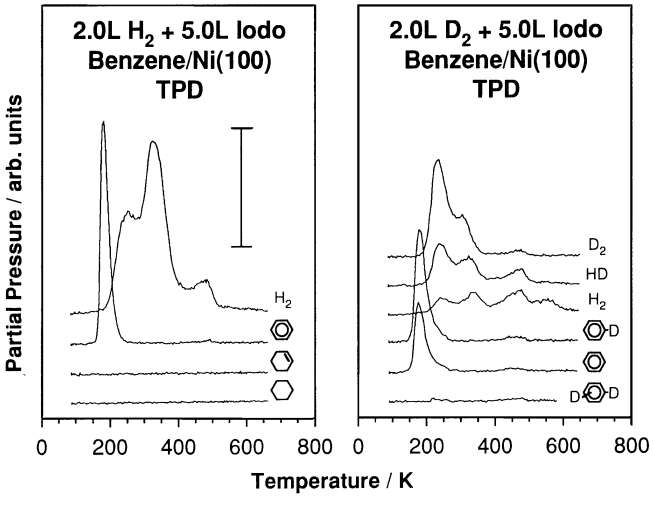

FIG. 10. Left: H_2, benzene, cyclohexene, and cyclohexane TPD spectra from a Ni(100) surface dosed sequentially with 2.0 L of hydrogen and 5.0 L of iodo benzene. Right: H_2, HD, D_2, and benzene (C_6H_5D, C_6H_6, and $C_6H_4D_2$) TPD spectra from a Ni(100) surface dosed sequentially with 2.0 L of deuterium and 5.0 L of iodo benzene. All dosings were done at 90 K.

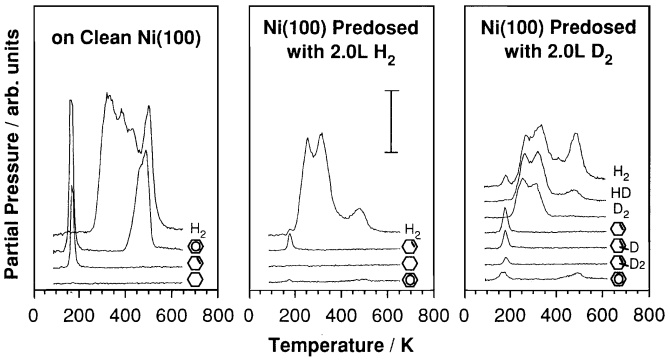

FIG. 11. H_2, benzene, cyclohexene, and cyclohexane TPD spectra from Ni(100) surfaces dosed with 5.0 L of 3-bromo cyclohexene (C_6H_9Br) (left) and 2.0 L H_2 + 5.0 L C_6H_9Br (center); and H_2, HD, D_2, cyclohexene (C_6H_{10}, C_6H_9D, and $C_6H_8D_2$), and benzene TPD spectra from a Ni(100) surface dosed with 2.0 L D_2 + 5.0 L C_6H_9Br (right). All dosings were done at 90 K.

Fig. 11 shows that a 5.0 L dose of 3-bromo cyclohexene generates both benzene and cyclohexene (in addition to hydrogen), but no cyclohexane. Benzene desorbs in two stages around 165 and 480 K, while cyclohexene comes off only at 165 K. This behavior resembles somewhat that of cyclohexene, but differs significantly from the one observed for the cyclohexadienes. The desorption of H_2 is seen in a broad and complex feature that covers a temperature range from 300 to 500 K. The effect of coadsorbed hydrogen and deuterium are shown in the center and right panels of Fig. 11, respectively. The preadsorption of 2.0 L H_2 causes the benzene to disappear almost completely, so only cyclohexene (180 K) and hydrogen (260 and 320 K) desorb with any significant yield. The presence of coadsorbed deuterium also generates some deuterium-containing cyclic products, specifically monodeutero- and dideutero-cyclohexene, around 175 K; the former clearly comes from recombination of cyclohexenyl species with surface deuterium, but the latter is quite probably produced by previous H–D exchange on the allylic species via the sequential formation of cyclohexene and allyl intermediates. Exchange on monodeutero-cyclohexene is expected at higher temperatures (see Fig. 2).

4. DISCUSSION

In order to develop a complete picture of the chemistry of cyclic hydrocarbons on Ni(100) surfaces, TPD studies on the thermal reactions of cyclohexane, cyclohexene, benzene, 1,3- and 1,4-cyclohexadienes, 1-methyl-1-cyclohexene, and toluene were combined with those on iodo cyclohexane, iodo benzene, and 3-bromo cyclohexene. Our previous work with C_1–C_6 straight and branched alkyl iodides has shown that the adsorption of alkyl iodides below 100 K is molecular but that the cleavage of the C–I bond, which requires an activation energy of only 2–4 kcal/mol, occurs

readily below 200 K (33, 35, 37, 43), and the main product resulting from this C–I bond dissociation is the corresponding surface alkyl species. We believe that the same process also occurs with cyclic halo hydrocarbons. The TPD experiments with both iodo cyclohexane and iodo benzene coadsorbed with deuterium, for example, lead to the formation of the corresponding monodeutero-cyclohexane and benzene molecules, respectively, and this presumably occurs via the direct reductive elimination of the cyclohexyl or phenyl groups with surface deuterium. The use of halides of cyclic compounds in this work allowed for the preparation of the most likely intermediates in the hydrogenation-dehydrogenation reactions of cyclic compounds in Ni(100) surfaces.

By combining studies using stable C_6 cyclic compounds (cyclohexane, cyclohexene, 1,3- and 1,4-cyclohexadiene, and benzene) with work with the halo compounds precursors for the preparation of the key intermediates (iodo cyclohexane, 3-bromo-1-cyclohexene, and iodo benzene), it was therefore possible to probe almost all the elementary surface steps involved in the interconversion of these hydrocarbon moieties on the Ni(100) surface. The final analysis of the data obtained here for Ni(100) is however somewhat complicated by three factors, namely: (1) most of the reactions of interest occur readily at low temperatures, and that makes the separation of each individual step in complex reactions quite difficult; (2) the detection of some of the compounds in TPD is limited by their desorption, not by the surface reactions that produce them; and (3) the desorption temperatures measured in TPD are in many instances severely affected by changes in surface coverages. Nevertheless, some clear conclusions could be derived from the results of this work. Scheme I summarizes the main observations from the experiments reported above, and will be used to guide our subsequent discussion.

We begin by looking at the chemistry of cyclohexane on Ni(100). The TPD results from that compound indicate that molecular desorption is preferred over surface decomposition. Cyclohexane has in fact already been reported to adsorb weakly on nickel via a van der Waals-type interaction [6] and to lie flat on Ni(111) (7). This is not surprising given the high stability of saturated hydrocarbons, even though some decomposition has been reported for cyclohexane on platinum surfaces (44–46). Specifically, the formation of a dehydrogenated intermediate, proposed to be a C_6H_9 allylic moiety, has been reported on Pt(111) around 180 K (45, 46). This pathway seems to not be operational on Ni(100). It is important to note, however, that cyclohexane can be clearly activated by nickel under catalytic conditions (47, 48), and that our inability to detect any dissociative adsorption here is most likely due to the dynamic nature of the TPD technique, which makes all cyclohexane desorb molecularly before reaching the temperatures needed for C–H bond activation. Since the most likely first intermediate from this activation is a cyclohexyl moiety, we have therefore performed independent experiments with that species, which was prepared by thermal treatment of adsorbed iodo cyclohexane. The cyclohexyl species generated after the C–I bond dissociation in these experiments mainly undergo dehydrogenation via a β-hydride elimination step to form cyclohexene, which either desorbs or remains on the surface and dehydrogenates further to benzene. Concurrently, cyclohexyl moieties can also be hydrogenated via recombination with hydrogen atoms generated either from background adsorption or from the decomposition of some of the cyclohexyl species to cyclohexane. The occurrence of this latter reductive elimination reaction was corroborated by experiments with coadsorbed deuterium, where it was seen that a significant amount of monodeutero-cyclohexane is indeed produced. A small amount of dideutero-cyclohexane is also made in those experiments, but that product desorbs at somewhat higher temperatures and is the result of a H–D exchange reaction that will be discussed in more detail later.

The next logical intermediate in the sequential dehydrogenation of cyclohexane is cyclohexene. When thermally activating cyclohexene adsorbed directly on Ni(100), only benzene and hydrogen are produced in large quantities. Almost no cyclohexane can be detected in this case, even if hydrogen is preadsorbed on the surface. This means that the energy barrier for going from cyclohexene to cyclohexane (in fact, to cyclohexyl, because hydrogenation of cyclohexyl to cyclohexane occurs readily) is somewhat higher than those for dehydrogenation and molecular desorption. Nevertheless, that difference cannot be too large, because the small amount of H–D exchange observed in cyclohexyl species most likely occurs via its reversible conversion to cyclohexene. Small signals for exchanged cyclohexane are indeed detected around or above 200 K in TPD experiments with either cyclohexene or iodo cyclohexane on deuterium-predosed surfaces.

The dehydrogenation of cyclohexene always gives benzene in high yields. This reaction has been proposed to proceed via the formation of cyclohexadiene (6), but quite likely involves the previous formation of a C_6H_9 allylic species. Indeed, this latter reaction is facile in organometallic compounds, because the allylic C–H bond is quite weak, about 20 kcal/mol weaker than the vinylic C–H bond (27). Both laser-induced desorption and bismuth postdosing experiments with cyclohexane and cyclohexene on Pt(111) have provided convincing proof for the formation of this allylic species on that surface (18, 45, 46). Evidence for allyl formation on nickel comes from the observation of some desorption of H–D-exchanged cyclohexene at 185 K from a surface dosed with deuterium and normal cyclohexane, since this exchange most likely takes place via the reversible dehydrogenation to a cyclohexenyl surface species (if it were to involve a cyclohexyl, that moiety would

hydrogenate readily to cyclohexane). The C_6H_9 intermediate was also prepared directly by thermally decomposing 3-bromo cyclohexene on the nickel substrate. Further thermal activation of that species produces both cyclohexene and benzene, but no cyclohexane. In fact, the conversion of the allyl intermediate to cyclohexene must be fast, because the TPD results from 3-bromo cyclohexene resemble quite closely those from the olefin. Last, it is interesting to point out that, in contrast with the case of cyclohexene, no toluene desorption is seen from 1-methyl-1-cyclohexene. This may be due to the fact that the C–H bonds in the methyl group are the weakest and most accessible in that case, so dehydrogenation may occur via the formation of either an allyl or a carbene intermediate involving the methyl carbon.

Allyl compounds, once formed, are expected to dehydrogenate readily via the formation of cyclohexadiene. The chemistry of both 1,3- and 1,4-cyclohexadienes was therefore studied here as well. It was found that 1,3-cyclohexadiene is more reactive than 1,4-cyclohexadiene, as expected; while the former dehydrogenates to benzene below 170 K, the latter requires about 25 K higher temperature to follow the same reaction. Since the formation of benzene from the allylic intermediate (in fact, from 3-bromo cyclohexene) starts below 165 K, it is therefore reasonable to assume that such a reaction does not involve 1,4-cyclohexadiene. We propose the formation of 1,3-cyclohexadiene as an intermediate between the allylic moiety and benzene. Unfortunately, this hypothesis could not be tested directly here, because under no circumstances could the desorption of cyclohexadiene be detected by TPD in any of the experiments described above.

Cyclohexadienes can be hydrogenated in the presence of surface hydrogen (or deuterium) as well. In organometallic compounds the migratory insertion of conjugated dienes into metal–hydrogen bonds (the reaction responsible for hydrogenation) is normally much easier than with simple olefins because of the formation of stable π-allylic complexes (27). In this work it was seen that the hydrogenation of 1,3-cyclohexadiene on Ni(100) occurs below 185 K and yields a small amount of cyclohexene. Given that cyclohexene formation from the allylic intermediate occurs at lower temperatures, however, it is concluded that the conversion of cyclohexadiene to cyclohexene is most likely limited by the incorporation of the first hydrogen; this indicates that the allyl may not be very stable. An additional complication arises from the fact that there are two possible isomers for the allylic species, namely, a σ (cyclohex-2-en-1-yl) and a π (η^3-cyclohexenyl) coordinated species. These two isomers usually exist in equilibrium, but the π-bonded complex is often the most stable. No direct information can be extracted from our experiments about this, but, based on previous work, we propose the adsorbed allyl species in the C_6 cyclic hydrocarbon case to be in a π configuration, and to be about as stable as the cyclohexyl moiety.

Next, cyclohexadienes dehydrogenate easily to benzene, as mentioned above. Even though this happens with both 1,3- and 1,4-intermediates, according to the TPD experiments reported here the reaction is significantly easier with the 1,3 conjugated compound. The dehydrogenation of 1,3-cyclohexadiene to benzene is in fact very efficient, as evidenced not only by the low temperature of the reaction ($<$170 K), but also by the high yields obtained. No intermediate was detected for this reaction, even though it involves the removal of two hydrogen atoms.

The chemistry of benzene on transition metal surfaces has been studied in great detail in the past (27, 49). On Ni(100) and at low coverages, benzene adsorbs with the ring parallel to the surface plane, with the benzene π orbitals lying above the nickel atoms, but at higher coverages the additional benzene rings force all molecules to reorient into a tilted geometry (2). As a consequence, two very separate features are seen for the molecular desorption of benzene: one around 165 K, associated with the "compressed" high-coverage layer, and another about 480 K, associated with the flat-lying benzene that results after desorption of about half of the initial amount of adsorbate molecules. This behavior has been seen on other surfaces as well, and has been nicely simulated with a Monte Carlo algorithm [50]. The fact that benzene desorbs in two temperature regimes allows for a qualitative determination of the amount of benzene that is produced by dehydrogenation of the other C_6 cyclic compounds studied here: the more benzene produced, the more intense the signal in the low temperature peak of the benzene trace of the TPD. Based on this idea it is easy to see that the dehydrogenation of cyclohexadienes and cyclohexenyl moieties are particularly facile reactions, while that of cyclohexene and cyclohexyl species competes somewhat unfavorably with hydrogenation and molecular desorption steps.

Finally, some chemisorbed benzene dehydrogenates on the surface to ultimately yield surface carbon and hydrogen. This is a high temperature reaction, because the resulting hydrogen is observed in TPD experiments only above 300 K. Furthermore, the H_2 TPD traces from cyclohexyl, cyclohexene, cyclohexenyl, and both cyclohexadienes, all display two main regions, one below 400 K, associated with the early dehydrogenation steps, and another around 470–500 K, due to benzene decomposition. This latter reaction presumably starts via the scission of one of the C–H aromatic bonds, which is about 110 kcal/mol strong, and leads to the formation of a phenyl intermediate. The chemistry of phenyl groups was probed here by using iodo benzene. Two main desorbing products were detected from TPD experiments with C_6H_5I, namely, benzene and hydrogen. The ease with which phenyl groups are hydrogenated to benzene (a reaction enhanced by the presence of coadsorbed hydrogen on the surface) points to a low activation barrier for that step, and the small but detectable amount of dideutero-

benzene seen in experiments with coadsorbed deuterium indicates that some (little) H–D exchange is possible in this case. On the other hand, the low temperature (<300 K) peak seen in the H_2 TPD shows that the dehydrogenation of the phenyl groups is fast. In fact, the low temperature H_2 TPD peak is desorption limited, so decomposition may occur at much lower temperatures; surface hydrogen is indeed available below 200 K for the formation of benzene. Finally, the thermal chemistry of toluene is somewhat different than that of benzene, because its decomposition probably starts at the methyl group; this is why hydrogen desorption is seen at low temperatures in this case (5, 27).

The TPD data discussed above can be used to get a semiquantitative picture of the energetics of the C_6 cyclic hydrocarbon conversion reactions on Ni(100) by using Hess-cycle arguments like those employed in the past for similar systems (33, 35, 51–53). Scheme II summarizes that information. There are significant error bars associated with the barriers shown in the energy diagram because of the uncertainty in the values used for the activation energies in these calculations, but these data can nevertheless be used to estimate general trends in reactivity for the surface species. For one, it is seen here that both cyclohexyl and cyclohexenyl surface species are less stable on Ni(100) than adsorbed cyclohexane, cyclohexene, or cyclohexadiene. It is interesting to note in particular that no special stability was seen here for cyclohexenyl on Ni(100), in contrast to what has been reported on Pt(111) (18, 45, 46). Furthermore, the estimated heat of formation for the cyclohexyl intermediate calculated here corresponds to a metal–carbon bond energy of about D(Ni-cyclohexyl) ~38 kcal/mol, a value in approximate agreement with the numbers reported previously for the bond energy of other chemisorbed alkyl groups: the metal–carbon bond for methyl and ethyl groups on nickel, platinum, copper, and iron are all on the order of 30 kcal/mol (27, 35, 34).

5. CONCLUSIONS

In the present work we have obtained results from temperature-programmed desorption experiments aimed at the characterization of the thermal chemistry of C_6 cyclic hydrocarbons (cyclohexane, cyclohexene, benzene, cyclohexadienes, 1-methyl-1-cyclohexene, and toluene) and halo hydrocarbons (iodo cyclohexane, iodo benzene, and 3-methyl-cyclohexene) on Ni(100) surfaces. The hydrogenation–dehydrogenation steps in C_6 cyclic hydrocarbon species on Ni(100) are summarized in Scheme I.

Iodo cyclohexane, which is believed to generate cyclohexyl species below 140 K, reacts much more readily on the Ni(100) surface than cyclohexane; while cyclohexane desorbs molecularly, cyclohexyl groups undergo β-hydride elimination to form cyclohexene (some of which dehydrogenates further to benzene) and reductive elimination with surface hydrogen to give cyclohexane. All this indicates that the cyclohexane is somewhat hard to activate on Ni(100) because of the ease with which it desorbs from the surface, but that it reacts easily via a sequence of hydrogenation and dehydrogenation steps once the first C–H bond is broken. Cyclohexene, which can be either produced by thermal

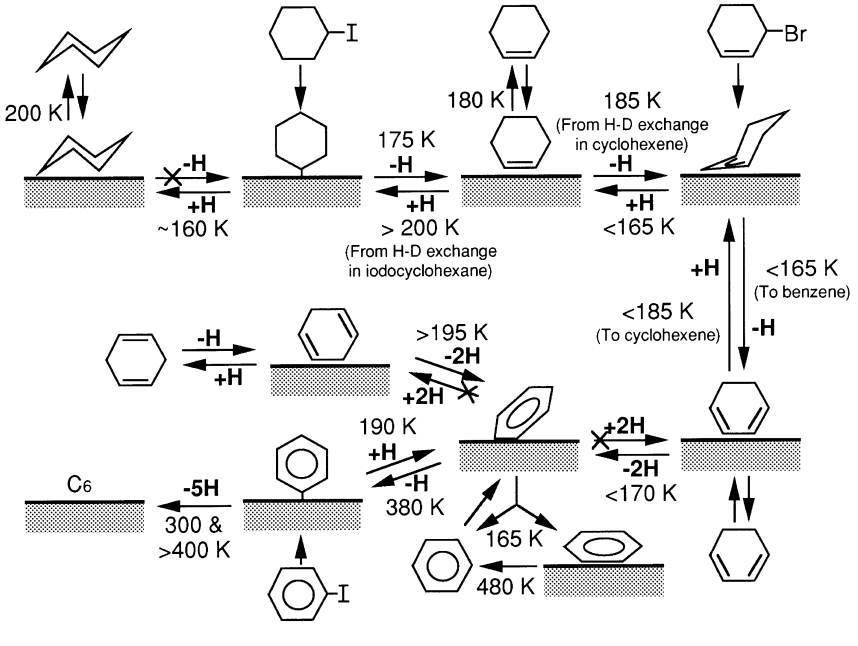

SCHEME I

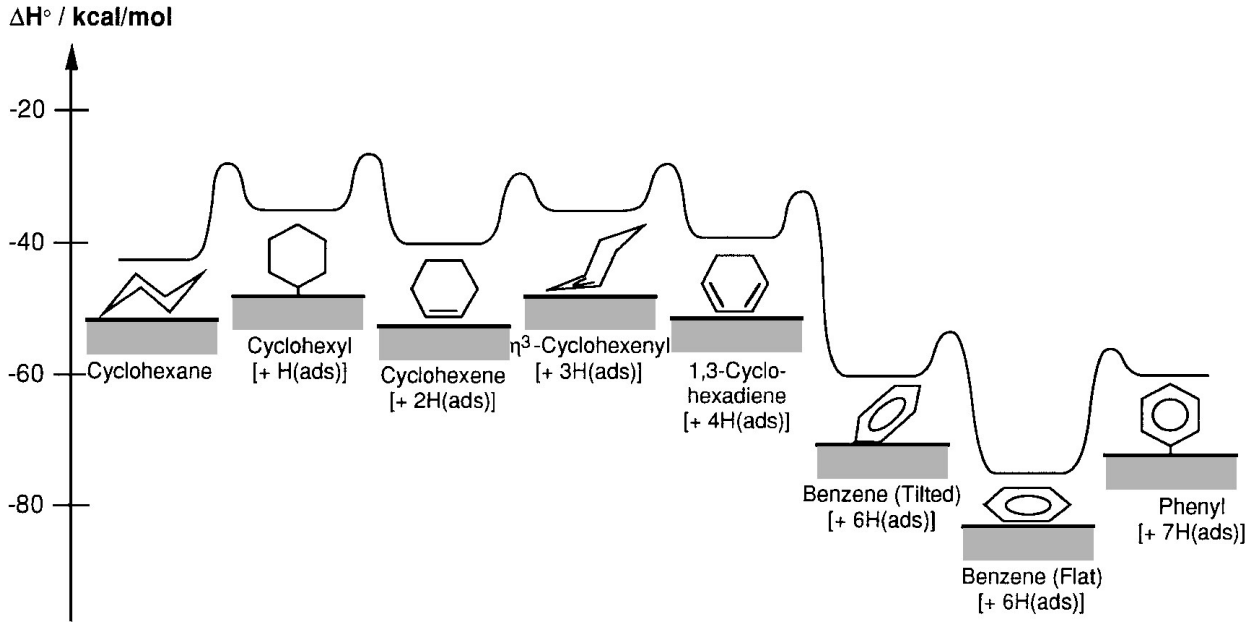

SCHEME II

activation of iodo cyclohexane or directly adsorbed on the surface, dehydrogenates preferentially to benzene, even though in the presence of surface deuterium it also exchanges at least one hydrogen atom from the ring. 3-Bromo cyclohexene also dehydrogenates readily to benzene, indicating that an allylic species may be involved in the first step of the cyclohexene dehydrogenation. 1,3-Cyclohexadiene is the most likely species to form next in that path. Benzene adsorption is partially reversible, especially at high coverages, where a compressed layer of rings in a tilted geometry is formed, but some of the flat-lying benzene does decompose at high temperatures. The thermal decomposition of both benzene and iodo benzene produce a surface phenyl intermediate which can be hydrogenated in the presence of coadsorbed hydrogen, but this reaction occurs at different temperatures in each case: the benzene formed by hydrogenation of a phenyl group created by iodo benzene decomposition desorbs at lower temperatures than when starting from adsorbed benzene on clean Ni(100), most likely because the phenyl moieties are produced at higher temperatures in the latter case. 1-methyl-1-cyclohexene reacts dissociatively to yield hydrogen but no toluene, presumably because of a change in reaction selectivity, as compared to the case of cyclohexene. Finally, hydrogen (or deuterium) coadsorption was found to enhance hydrogenation and H–D exchange reactions in some cases, but not in others. For instance, the presence of coadsorbed hydrogen (or deuterium) inhibits the formation of benzene from iodo cyclohexane but not H–D exchange, and when deuterium is coadsorbed with cyclohexene and 3-bromo cyclohexene the desorption of monodeutero- and dideutero-cyclohexene is observed, respectively, indicating that H–D exchange occurs in those cases as well. The energetics of all these reactions is summarized in Scheme II.

ACKNOWLEDGMENT

Financial support for this research was provided by a grant from the National Science Foundation (CHE-9530191).

REFERENCES

1. Steinruck, H.-P., Huber, W., Pache, T., and Menzel, D., *Surf. Sci.* **218**, 293 (1989).
2. Myer, A. K., Schoofs, G. R., and Benziger, J. B., *J. Phys. Chem.* **91**, 2230 (1987).
3. Bertolini, J. C., Dalmai-Imelik, G., and Rousseau, J., *Surf. Sci.* **67**, 478 (1977).
4. Bertolini, J. C., and Rousseau, J., *Surf. Sci.* **89**, 467 (1979).
5. Friend, C. M., and Muetterties, E. L., *J. Am. Chem. Soc.* **103**, 773 (1981).
6. Tsai, M.-C., Friend, C. M., and Muetterties, E. L., *J. Am. Chem. Soc.* **104**, 2539 (1982).
7. Zebisch, P., Huber, W., and Steinrnck, H.-P., *Surf. Sci.* **244**, 185 (1991).
8. Demuth, J. E., and Eastman, D. E., *Phys. Rev. B* **13**, 1523 (1976).
9. Huber, W., Steinrnck, H.-P., Pache, T., and Menzel, D., *Surf. Sci.* **217**, 103 (1989).
10. Lehwald, S., and Ibach, H., *Surf. Sci.* **89**, 425 (1979).
11. Demuth, J. E., and Eastman, D. E., *Phys. Rev. Lett.* **32**, 1123 (1974).
12. Blass, P. M., Akhter, S., and White, J. M., *Surf. Sci.* **191**, 406 (1987).
13. Rodriguez, J. A., and Campbell, C. T., *J. Catal.* **115**, 500 (1989).
14. Rodriguez, J. A., and Campbell, C. T., *J. Phys. Chem.* **93**, 826 (1989).
15. Land, D. P., Pettiette-Hall, C. L., McIver, R. T., Jr., and Hemminger, J. C., *J. Am. Chem. Soc.* **111**, 5970 (1989).
16. Tsai, M.-C., and Muetterties, E. L., *J. Am. Chem. Soc.* **104**, 2534 (1982).
17. Land, D. P., Erley, W., and Ibach, H., *Surf. Sci.* **289**, 237 (1993).
18. Henn, F. C., Diaz, A. L., Bussell, M. E., Hugenschmidt, M. B., Domagala, M. E., and Campbell, C. T., *J. Phys. Chem.* **96**, 5965 (1992).
19. Hoffmann, F. M., Felter, T. E., Thiel, P. A., and Weinberg, W. H., *Surf. Sci.* **130**, 173 (1983).

20. Madey, T. E., and Yates, J. T., Jr., *Surf. Sci.* **76**, 397 (1978).
21. Nishijima, M., Fujisawa, M., Takaoka, T., and Sekitani, T., *Surf. Sci.* **283**, 121 (1993).
22. Raval, R., and Chesters, M. A., *Surf. Sci.* **219**, L505 (1989).
23. Raval, R., Pemble, M. E., and Chesters, M. A., *Surf. Sci.* **210**, 187 (1989).
24. Chesters, M. A., Parker, S. F., and Raval, R., *Surf. Sci.* **165**, 179 (1986).
25. Zaera, F., *Acc. Chem. Res.* **25**, 260 (1992).
26. Zaera, F. J., *Mol. Catal.* **86**, 221 (1994).
27. Zaera, F., *Chem. Rev.* **95**, 2651 (1995).
28. Zhou, X.-L., Zhu, X.-Y., and White, J. M., *Acc. Chem. Res.* **23**, 237 (1990).
29. Zaera, F., *Surf. Sci.* **219**, 453 (1989).
30. Zaera, F., *Surf. Sci.* **262**, 335 (1992).
31. Zaera, F. J., *Am. Chem. Soc.* **111**, 8744 (1989).
32. Zaera, F., and Hoffmann, H., *J. Phys. Chem.* **95**, 6297 (1991).
33. Tjandra, S., and Zaera, F., *Langmuir* **8**, 2090 (1992); **9**, 880 (1993).
34. Tjandra, S., and Zaera, F., *J. Catal.* **144**, 361 (1993).
35. Tjandra, S., and Zaera, F., *Surf. Sci.* **289**, 255 (1993).
36. Tjandra, S., and Zaera, F., *Surf. Sci.* **322**, 140 (1995).
37. Tjandra, S., and Zaera, F., *Langmuir* **10**, 2640 (1994).
38. Tjandra, S., and Zaera, F., *J. Catal.* **147**, 598 (1994).
39. Zaera, F., and Tjandra, S., *J. Phys. Chem.* **98**, 3044 (1994).
40. Zaera, F., and Tjandra, S., *J. Am. Chem. Soc.* **115**, 5851 (1993).
41. Tjandra, S., and Zaera, F., *J. Am. Chem. Soc.* **114**, 10645 (1992).
42. Redhead, P. A., *Vacuum* **12**, 203 (1962).
43. Tjandra, S., and Zaera, F., *J. Am. Chem. Soc.* **117**, 9749 (1995).
44. Blakely, D. W., and Somorjai, G. A., *J. Catal.* **42**, 181 (1976).
45. Pettiette-Hall, C. L., Land, D. P., McIver, R. T., Jr., and Hemminger, J. C., *J. Am. Chem. Soc.* **113**, 2755 (1991).
46. Bussell, M. E., Henn, F. C., and Campbell, C. T., *J. Phys. Chem.* **96**, 5978 (1992).
47. Kemball, C., *Adv. Catal.* **11**, 223 (1959).
48. Anderson, J. R., and Baker, B. G., *in* "Chemisorption and Reaction on Metallic Films" (J. R. Anderson, Ed.), Chap. 8, pp. 63–210, Academic Press, London (1971).
49. Netzer, F. P., and Ramsey, M. G., *Crit. Rev. Solid Mater. Sci.* **17**, 397 (1992).
50. Tysoe, W. T., *Langmuir* **12**, 78 (1996).
51. Zaera, F., *J. Phys. Chem.* **94**, 5090 (1990).
52. Zaera, F., *J. Phys. Chem.* **94**, 8350 (1990).
53. Zaera, F., *Langmuir* **12**, 88 (1996).
54. Tjandra, S., and Zaera, F., *Langmuir* **9**, 880 (1993).